JACC: CLINICAL ELECTROPHYSIOLOGY VOL. 7, NO. 5, 2021

PUBLISHED BY ELSEVIER

Electroanatomic Characterization and Ablation of Scar-Related Isthmus Sites Supporting Perimitral Flutter

George Katritsis, MBChB,[a] Vishal Luther, PhD,[a] Nuno Cortez-Dias, MD,[b] Luís Carpinteiro, MD,[b] João de Sousa, MD,[b] Phang Boon Lim, PhD,[a] Zachary Whinnett, PhD,[a] Fu Siong Ng, PhD,[a] Michael Koa-Wing, PhD,[a] Norman Qureshi, PhD,[a] Anthony Chow, PhD,[c] Sharad Agarwal, MD,[d] Shahnaz Jamil-Copley, PhD,[e] Nicholas S. Peters, MD,[a] Nick Linton, PhD,[a] Prapa Kanagaratnam, PhD[a]

ABSTRACT

OBJECTIVES The authors reviewed 3-dimensional electroanatomic maps of perimitral flutter to identify scar-related isthmuses and determine their effectiveness as ablation sites.

BACKGROUND Perimitral flutter is usually treated by linear ablation between the left lower pulmonary vein and mitral annulus. Conduction block can be difficult to achieve, and recurrences are common.

METHODS Patients undergoing atrial tachycardia ablation using CARTO3 (Biosense Webster Inc., Irvine, California) were screened from 4 centers. Patients with confirmed perimitral flutter were reviewed for the presence of scar-related isthmuses by using CARTO3 with the ConfiDense and Ripple Mapping modules.

RESULTS Confirmed perimitral flutter was identified in 28 patients (age 65.2 ± 8.1 years), of whom 26 patients had prior atrial fibrillation ablation. Scar-related isthmus ablation was performed in 12 of 28 patients. Perimitral flutter was terminated in all following correct identification of a scar-related isthmus using ripple mapping. The mean scar voltage threshold was 0.11 ± 0.05 mV. The mean width of scar-related isthmuses was 8.9 ± 3.5 mm with a conduction speed of 31.8 ± 5.5 cm/s compared to that of normal left atrium of 71.2 ± 21.5 cm/s ($p < 0.0001$). Empirical, anatomic ablation was performed in 16 of 28, with termination in 10 of 16 (63%; $p = 0.027$). Significantly less ablation was required for critical isthmus ablation compared to empirical linear lesions (11.4 ± 5.3 min vs. 26.2 ± 17.1 min; $p = 0.0004$). All 16 cases of anatomic ablation were reviewed with ripple mapping, and 63% had scar-related isthmus.

CONCLUSIONS Perimitral flutter is usually easy to diagnose but can be difficult to ablate. Ripple mapping is highly effective at locating the critical isthmus maintaining the tachycardia and avoiding anatomic ablation lines. This approach has a higher termination rate with less radiofrequency ablation required. (J Am Coll Cardiol EP 2021;7:578–90)

Perimitral flutter (PMF) is a common atrial tachycardia (AT) encountered in patients following left atrial (LA) catheter ablation, after cardiac surgery, and with cardiomyopathies associated with LA scar (1,2). A rapid diagnosis can be made by mapping the post-pacing intervals from catheters within the coronary sinus (CS) and at an anterior LA mitral site. Catheter ablation of PMF involves endocardial ablation to create a line of conduction block at the typical mitral isthmus (MI), which transects the macro-re-entrant PMF circuit (3,4). However, conduction block of the typical MI is challenging to achieve. Even when additional epicardial radiofrequency (RF) ablation is performed via the CS, rates

From the [a]Imperial College Healthcare, London, United Kingdom; [b]Hospital de Santa Maria, Lisbon, Portugal; [c]Barts Heart Centre, London, United Kingdom; [d]Papworth Hospital, Cambridge, United Kingdom; and the [e]Nottingham University Hospitals, Nottingham, United Kingdom.
The authors attest they are in compliance with human studies committees and animal welfare regulations of the authors' institutions and Food and Drug Administration guidelines, including patient consent where appropriate. For more information, visit the Author Center.

Manuscript received September 3, 2020; revised manuscript received October 24, 2020, accepted October 24, 2020.

ISSN 2405-500X/$36.00 https://doi.org/10.1016/j.jacep.2020.10.017

of conduction block as low as 60% to 70% are reported (4,5). As a result, alternative approaches to catheter ablation of PMF lesions have been described and most commonly involve linear ablation of the anterior LA wall (6–9). Despite improved acute success rates by anterior LA wall ablation, recurrence rates after any linear lesion remain between 40% and 50% (9). Ablation of a constrained isthmus site supporting the macro-re-entrant circuit are often quoted as the most favorable sites for ablation (10,11). However, there are limitations to the current mapping approaches used to identify these sites.

Ripple mapping (RM) is a 3-dimensional (3D) electroanatomic approach on the CARTO platform that allows simultaneous assessment of activation and voltage (12–16). We have previously demonstrated the superiority of RM over conventional local activation time (LAT) mapping in a multicenter randomized controlled trial (17). This superiority was partly consequent to operators identifying constrained, LA scar-related isthmus sites during tachycardia when using RM. We reviewed data from PMF cases performed using RM or LAT mapping to determine whether there was evidence of constrained isthmus in PMF cases and whether this was influenced by the mapping methods.

SEE PAGE 591

METHODS

We conducted a multicenter review of catheter ablation procedures for PMF from 4 sites. Patients undergoing catheter ablation for PMF, performed on the CARTO3 (Biosense Webster Inc., Irvine, California) mapping platform with the ConfiDense continuous mapping module, using a multipolar mapping catheter (PentaRay or Lasso, Biosense Webster Inc.), were included. The ConfiDense module ensures automatic point acquisition against predefined electrogram (EGM) activation time, morphology, and electrode proximity filters. RF ablation was delivered by the SmartTouch Thermocool catheter (Biosense Webster Inc.) via a Stockert generator (Biosense Webster Inc.). All procedures were carried out following local protocols with regard to mode of sedation/anesthesia, exclusion of LA appendage thrombus, and transseptal puncture.

DEFINITIONS OF PMF, CRITICAL ISTHMUS SITES, AND LA SCAR.

Perimitral flutter.

- Ripple map: A continuous sequence of ripple bars demonstrating LA activation rotating around the mitral annulus.
- LAT map: Isochrones demonstrating a continuous sequence of LA activation around the mitral annulus, with earliest activation adjacent to latest activation. The range of mapped LAT in the LA had to include >90% of the total tachycardia cycle length.

Scar-related RM isthmus site.

- An area of LA tissue where conduction slowing could be appreciated on the RM.
- This area of atrial tissue had to be bordered by nonconducting tissue (scar tissue or anatomic obstacle).
- Recorded bipolar EGMs demonstrating fractionation.

All isthmuses were defined over an 8-segment model of the LA (1: anterior; 2: lateral; 3: LA appendage; 4: roof; 5: posterior; 6: typical MI; 7: floor; 8: septum).

The conduction speed of the scar-related RM isthmus, during tachycardia, was determined by the following method. Individual mapped points at the entry and exit of the RM isthmus were marked on the LA geometry as a ripple marking. The EGM of each ripple marking was displayed in the Ripple Viewer of CARTO3. The time difference between the entry and exit EGM was determined by using digital time calipers in the Ripple Viewer. The distance between the entry and exit points on the LA geometry was measured by using the distance measurement function on the CARTO3 platform. Conduction speed (cm/s) was calculated as distance (cm) divided by time (s). The average of 3 EGM entry/exit pairs per individual isthmus was taken as the conduction speed of an RM isthmus. To determine the conduction speed of the healthy LA during tachycardia, this process was performed at a site of normal-voltage, passively activating LA tissue.

SCAR TISSUE. Scar tissue was defined as mapped LA tissue where there was no discernible electrical activity above baseline noise, as previously described (13). This process is based on the ability to visualize activation and bipolar voltage simultaneously on a single 3D LA geometry using RM. The bipolar voltage threshold for the atrium was established when all areas designated as scar contained no ripple bars (i.e., are nonconducting) or the ripple bars had no propagative relationship. In CARTO3, this will lead to all sites with a bipolar voltage equal to or less than the ripple voltage threshold (nonconducting areas) as red or scar. Any voltage above the ripple

ABBREVIATIONS AND ACRONYMS

3D = 3-dimensional
AT = atrial tachycardia
CS = coronary sinus
EGM = electrogram
LA = left atrium
LMIL = lateral mitral isthmus line
MI = mitral isthmus
PMF = perimitral flutter
RF = radiofrequency
RM = ripple mapping
SMIL = septal mitral isthmus line

FIGURE 1 Ripple Voltage Thresholding

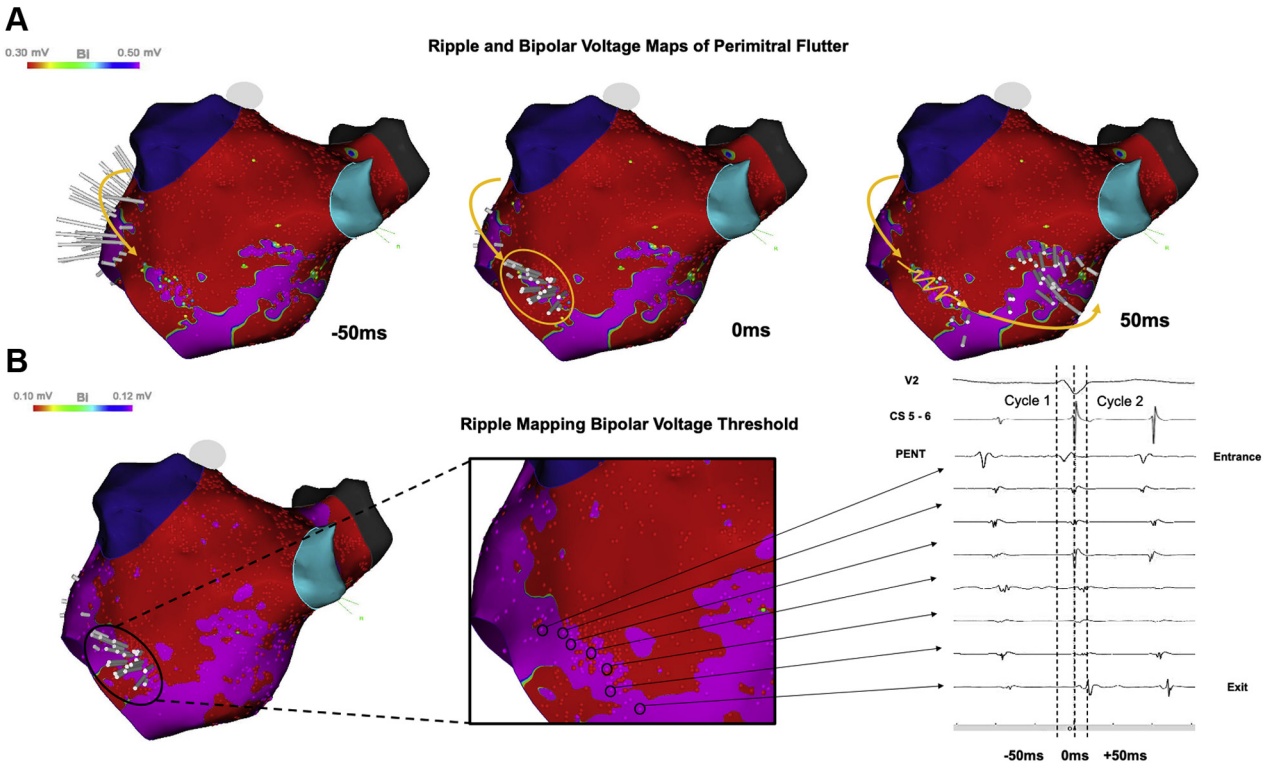

(A) An arbitrary LA bipolar voltage threshold of 0.30 to 0.50 mV is selected. Frames of the RM collected during PMF are displayed at -50 ms, 0 ms, and 50 ms around the reference signal, CS 5 to 6. Yellow arrows show the direction of activation. Encircled is an area of ripple bars demonstrating activation within scar **(red)** from previous LMIL ablation. **(B)** Lowering the LA bipolar voltage limits for the map so that the encircled area of ripple bars is displayed as conducting LA tissue **(purple)** and defines a threshold of 0.10 mV. A scar-related isthmus can be seen as a gap in the previous ablation line (Video 1). Fractionated EGMs from within the isthmus are shown. The isthmus contains 87 ms of this 270-ms tachycardia. CS = coronary sinus; EGM = electrogram; LA = left atrium; PENT = PentaRay catheter; PMF = perimitral flutter; RM = ripple mapping.

threshold will appear purple. Potential scar-related isthmuses, therefore, become more apparent (**Figure 1** and Video 1). To determine the mean bipolar voltage of the scar-related isthmus itself, 3 points at the entry and exit of each isthmus where selected, and the bipolar voltage amplitude mean values of all 6 were recorded.

ABLATION STRATEGY AND OUTCOMES. The ablation strategy and outcome for each case was determined by assessment of the ablation lesions on the electroanatomic maps, intracardiac EGM recordings, and procedural reports. Ablation strategies were categorized into 2 groups:

Linear ablation of anatomic MI sites.

- Lateral MI line (LMIL): from the inferior left lower pulmonary vein (LLPV) to the lateral mitral annulus (9).
- Septal MI line (SMIL): from the right upper pulmonary vein (RUPV) diagonally to the anterior mitral annulus (9).

Scar-related isthmus ablation.

- Constrained ablation to a scar-related isthmus site only.

Ablation outcomes were defined as follows:

- Successful ablation: ablation leading to PMF termination or change.
- Unsuccessful ablation: ablation unable to terminate or change tachycardia (external cardioversion required to restore sinus rhythm).

Where ablation lesions were performed, rates of conduction block were documented. Conduction block could be demonstrated by remapping the LA during an atrial paced rhythm or by performing differential pacing maneuvers.

STATISTICAL ANALYSIS. Categorical variables are expressed as percentages; continuous variables are expressed as mean ± 1 SD for parametric data and/or median (lower quartile to upper quartile) for nonparametric data. Categorical data were analyzed using either a Fisher exact test or chi-square test where appropriate. Unpaired data were analyzed using a Student's *t*-test for parametric data and Mann-Whitney *U* test for nonnormal data. A 2-sided p value was determined where applicable, and a value of $p \leq 0.05$ was considered significant.

RESULTS

PATIENT AND PROCEDURAL CHARACTERISTICS. A total of 43 catheter ablation procedures were identified that had been treated as PMF by using the CARTO system. Of these, 15 cases were excluded: 11 for missing data and 4 for unreliable diagnosis of PMF. Therefore, 28 eligible patients with PMF were included for analysis. The clinical procedures for the 28 included patients were performed by using an RM and/or LAT mapping at the operator's discretion.

The mean patient age was 65.2 ± 8.1 years, and 20 patients were male. Catheter ablation for AF with wide area circumferential ablation had previously been performed in 26 of 28 (92%). A history of previous linear ablation targeting an anatomic MI (lateral or septal) was documented in 12 of 28 (43%) of patients. Of these patients, 11 had previously documented LMIL ablation, and 3 had SMIL ablation.

All patients were in stable AT on the day of the procedure, and a decapolar recording catheter was inserted in the CS in all. The diagnosis of PMF circuit was made by 3D electroanatomic mapping alone or in combination with entrainment. In 21 of 28 (75%), the initial rhythm was PMF, and in 7 of 28, the initial rhythm was a different AT, which became stable PMF after ablation. A dual-loop circuit was diagnosed on the basis of the electroanatomic map in 5 of 28 (18%), with 1 loop around the annulus and the other around the LA roof in 3 patients, around the left pulmonary veins in 1 patient, and around an anterior wall scar in 1 patient. The mean PMF cycle length was 303.3 ± 131.7 ms, and the circuit was rotating in a counterclockwise direction in 15 of 28 (54%).

Multielectrode catheters were used for electroanatomic mapping in all patients: the PentaRay in 24 of 28 (85%) and the Lasso in 4 of 28 (15%). The mean number of points collected per electroanatomic map was 3,297 ± 1,285. RF energy was power controlled (25 to 35 W) and delivered to achieve ablation index targets between 500 and 550 for the anterior LA wall and between 400 and 450 for the posterior LA wall in all cases. No major procedural complications were recorded.

Baseline characteristics are summarized in **Table 1**.

SCAR-RELATED ISTHMUS ABLATION. In 12 patients, a scar-related isthmus site was identified as the optimal ablation site. These were all diagnosed with RM. Ablation of the scar-related isthmus was successful and led to PMF termination in all 12 patients. An example is shown in **Figure 2** and Video 2. Conduction block of the scar-related RM isthmus, by differential pacing or 3D electroanatomic remapping during LA pacing, was documented in 11 of 12 (92%).

Scar-related RM isthmus sites were narrow areas of LA tissue, with a mean width 8.9 ± 3.5 mm. Conduction through the isthmus was associated with a visual slowing of activation seen on the RM. Conduction speed of isthmus sites was 31.8 ± 15.5 cm/s, which was significantly lower than that of the normal LA conduction speed (71.2 ± 21.5 cm/s; $p < 0.0001$). Recorded bipolar EGMs were accordingly fractionated. The mean bipolar voltage threshold that defined activation of the isthmus was low, 0.11 ± 0.05 mV, as defined by the RM threshold of each tachycardia. LA tissue below this very low RM voltage threshold was defined as scar and always formed the functional boundaries of scar-related RM isthmus sites. The mean bipolar voltage of the scar-related isthmus itself was 0.30 ± 0.09 mV; that is to say, on average, tissue between 0.11 and 0.30 mV was indicative of a scar-related isthmus, tissue below 0.11 mV was indicative of scar, and tissue above 0.30 mV was healthy.

The scar-related RM isthmus could be categorized into gap related or non-gap related. Gap-related isthmuses (5 of 12) were bordered on both sides by LA scar arising from previous MI linear ablation (4 LMIL and 1 SMIL). Non-gap-related isthmuses where predominantly identified on the anterior LA wall segment (5 of 12). These sites were bordered superiorly by areas of scar tissue extending anteriorly from the LA roof and/or upper PVs. Interestingly, in 2 of 5 of these cases, this scar was idiopathic, and examples are shown in **Figure 3** and Video 3. The remaining 2 of 5 non-gap-related constrained isthmuses were at the typical anatomic MI LA segment in patients with previous atrial fibrillation ablation.

The mean number of RF energy applications in a scar-related RM isthmus was 11.2 ± 6.0 lesions, with a mean time of RF energy delivery of 11.4 ± 5.3 min per case.

To determine whether LAT mapping would have identified the isthmus in these 12 cases, we retrospectively reviewed these with an independent

TABLE 1 Patient and Procedural Characteristics

Patient #	Age, yrs	Ablation History	Cycle, ms	Direction	Points	Catheter	Ablation Strategy	Ablation Outcome	RM Isthmus
1	69	WACA + LMIL + SMIL	300	CC	3,967	PR	Isthmus	Termination	SMIL gap*
2	58	WACA	240	C	4,147	PR	Isthmus	Termination	Anatomic MI*
3	67	WACA + LMIL	310	C	3,888	PR	Isthmus	Termination	LMIL gap*
4	70	WACA	370	C	2,037	PR	Isthmus	Termination	Anterior LA wall*
5	61	WACA + LMIL	540	C	3,270	PR	Isthmus	Termination	LMIL gap*
6	74	WACA + LMIL	280	C	1,250	PR	Isthmus	Termination	LMIL gap*
7	66		500	C	5,359	L	Isthmus	Termination	Anterior LA wall*
8	68	WACA + LMIL + SMIL	270	CC	3,951	L	Isthmus	Termination	Anterior LA wall*
9	72	WACA	224	C	2,607	PR	Isthmus	Termination	Anatomic MI*
10	64	–	261	CC	4,149	PR	Isthmus	Termination	Anterior LA wall*
11	66	WACA + SMIL	277	CC	3,748	PR	Isthmus	Termination	Anterior LA wall*
12	61	WACA + LMIL	275	C	6,042	PR	Isthmus	Termination	LMIL gap*
13	57	WACA + LMIL	220	C	1,479	PR	LMIL + SMIL	Termination	Anterior LA wall†
14	76	WACA + LMIL	300	C	2,823	PR	LMIL (CS)	Termination	Posterior LA wall†
15	62	WACA	250	CC	5,678	PR	LMIL (CS)	DCCV	None
16	61	WACA	210	C	3,507	PR	LMIL	Changed to other AT	LPV carina†
17	67	WACA	270	CC	1,837	PR	LMIL	Changed to other AT	Anterior LA wall†
18	39	WACA	270	CC	1,890	PR	LMIL	Termination	LMIL gap†
19	72	WACA + LMIL	855	CC	3,910	PR	LMIL	Termination	Typical MI†
20	64	WACA	217	CC	3,099	PR	LMIL + SMIL	Termination	None
21	59	WACA	273	CC	3,648	L	SMIL	Termination	None
22	56	WACA + LMIL	230	CC	4,956	L	LMIL	DCCV	None
23	70	WACA	243	CC	2,960	PR	LMIL (CS)	Changed to other AT	None
24	77	WACA	260	CC	2,045	PR	SMIL	Termination	None
25	77	WACA	291	CC	3,315	PR	LMIL (CS)	Termination	Anterior LA wall†
26	62	WACA + LMIL	233	CC	1,369	PR	LMIL + SMIL	Termination	Anterior LA wall†
27	74	WACA	240	CC	2,150	PR	LMIL (CS)	Termination	Anterior LA wall†
28	58	WACA	180	CC	2,718	PR	LMIL + SMIL	Termination	LMIL gap†
Mean	65.2		303		3,279				

*Isthmus identified during clinical procedure. †Isthmus identified following retrospective RM analysis.

AT = atrial tachycardia; C = clockwise; CC = counterclockwise; CS = coronary sinus; DCCV = direct current cardioversion; L = lasso; LA = left atrium; LMIL = lateral mitral isthmus line; LPV = left pulmonary veins; MI = mitral isthmus; PR = PentaRay (Biosense Webster Inc., Irvine, California); RM = ripple mapping; SMIL = septal mitral isthmus line; WACA = wide area circumferential ablation.

clinical support specialist nominated by Biosense-Webster to determine if the same isthmus could be identified. This was possible for 8 of 12 (67%) of the isthmuses using the most up-to-date version of the system. Supplemental Figure 1 and Video 4 demonstrate the LAT map for the patient in **Figure 2**. Supplemental Figure 2 and Video 5 show a case where the LAT map fails to identify the scar-related isthmus, which is a true gap in a previous LMIL.

LINEAR ABLATION OF AN ANATOMIC MI. Sixteen patients had catheter ablation to deliver an MI line (LMIL or SMIL) for PMF. PMF was terminated by the first linear lesion attempted in 10 of 16 (63%). The first linear lesion was significantly less likely to terminate PMF than scar-related isthmus ablation ($p = 0.027$). Four patients required a second liner ablation to terminate PMF, raising the total cumulative success rate of linear lesions to 88%.

LMIL ablation was performed in the vast majority of cases, 14 of 16 (88%), and ablation of the SMIL in 5 of 16 (31%). Epicardial ablation via the CS was required for 5 of 16 LMIL ablations (50%). Conduction block across linear lesions was achieved in 11 of 16 (69%). All linear lesions where block was not achieved after the first attempt were remapped while pacing from a site within the LA. In 5 of 16 (31%), conduction block could not be achieved. A persisting "gap" of conduction block despite extensive ablation could be mapped in 2 of 5; subsequent ablation did not achieve block. Block could not be achieved in 4 LMILs (but CS ablation was not attempted in 2) and 1 SMIL. The rate of conduction block of an LMIL was, therefore, 71% and of an SMIL was 83%.

The length of a linear ablation lesion varied according to whether LMIL or SMIL ablation was performed. The mean length of an LMIL was 37.8 ± 6.0 mm and of an SMIL was 56.0 ± 8.4 mm ($p < 0.0001$). Both lines were also significantly ($p < 0.0001$) longer than a scar-related RM isthmus, contributing to the lesser amount of ablation required

FIGURE 2 Scar-Related Isthmus Ablation

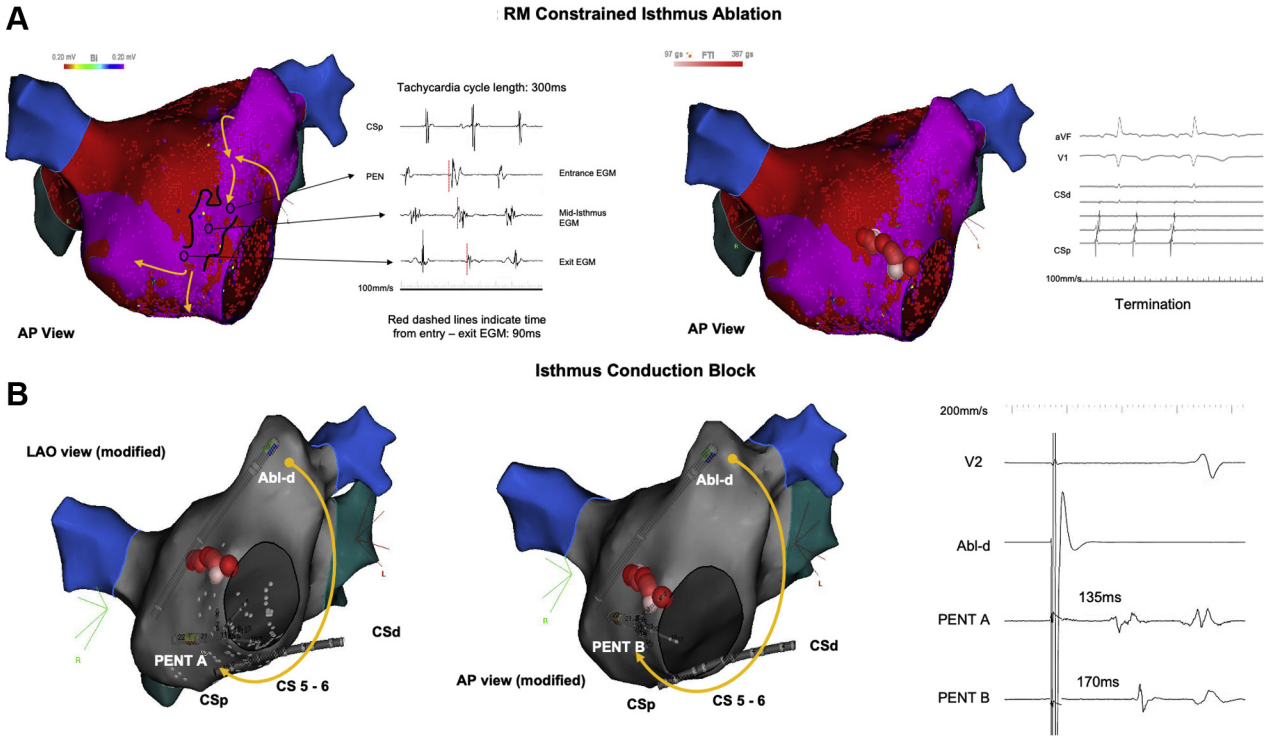

(A) LA bipolar voltage map collected during PMF after RM thresholding. The LA bipolar voltage threshold is established at 0.20 mV. **Orange arrows** indicate the direction of activation seen during review of the RM (Video 2). Fractionated EGMs from within the RM isthmus are shown. The isthmus contains 90 ms of this 300-ms tachycardia. Ablation of the RM isthmus terminates tachycardia (Video 2). **(B)** Pacing from the LAA (ablation catheter) after ablation. The mapping catheter is moved to the position PENT A, recording a delay of 135 ms from stimulation artifact to local EGM. The mapping catheter is then moved to the position PENT B, and the local EGM delays further to 190 ms, suggesting isthmus conduction block. Abl-d = ablation catheter - distal; AP = anteroposterior view; CSd = coronary sinus catheter - distal; CSp = coronary sinus catheter - proximal; LAA = left atrial appendage; LAO = left anterior oblique; other abbreviations as in Figure 1.

for the scar-related RM isthmus cases. For linear ablation, the mean RF applications per case were 30.8 ± 19, and the mean time of RF energy delivery 26.2 ± 17.1 min. Scar-related isthmus ablation was superior for both parameters; mean RF applications: 11.2 ± 6 versus 30.8 ± 19 ($p = 0.006$) and RF time: 11.4 ± 5.3 versus 26.2 ± 17.1 min ($p = 0.0004$).

Figure 4 illustrates examples of LMIL and SMIL ablation. Ablation outcomes are summarized in Table 2.

SCAR-RELATED ISTHMUS SITES WHERE LINEAR ABLATION WAS PERFORMED. The 16 cases where linear ablation of an anatomic MI was performed (16 of 28) were analyzed retrospectively to determine if a scar-related RM isthmus could be identified. It was possible to identify a scar-related RM isthmus in 10 of 16 (63%) cases.

Retrospective analysis of the 10 cases of linear ablation with a scar-related RM isthmus determined a similar RM bipolar voltage threshold (0.15 ± 0.01 mV) compared to the mean of the 12 cases (0.11 ± 0.05 mV), where a scar-related RM isthmus was ablated at the index procedure ($p > 0.05$). Similarly, the mean width of the 10 retrospectively identified scar-related RM isthmuses was narrow (9.09 ± 8.6 mm), and the conduction speed was 36.0 ± 14.9 cm/s ($p > 0.05$).

The functional borders that defined the 10 retrospectively identified scar-related RM isthmus sites were also formed by LA scar tissue. Scar tissue was either a result of previous linear ablation of the LA, giving rise to a gap-related RM isthmus (2 of 10), or due to anterior wall scar (5 of 10) in a similar distribution to that observed in the 12 cases where ablation of the scar-related isthmus led to PMF termination. We retrospectively identified 1 RM constrained isthmus at the typical MI segment of the LA. Atypical scar-related RM isthmus locations were observed in 2 cases (posterior LA wall segment and left pulmonary vein carina).

FIGURE 3 PMF Without Previous Ablation

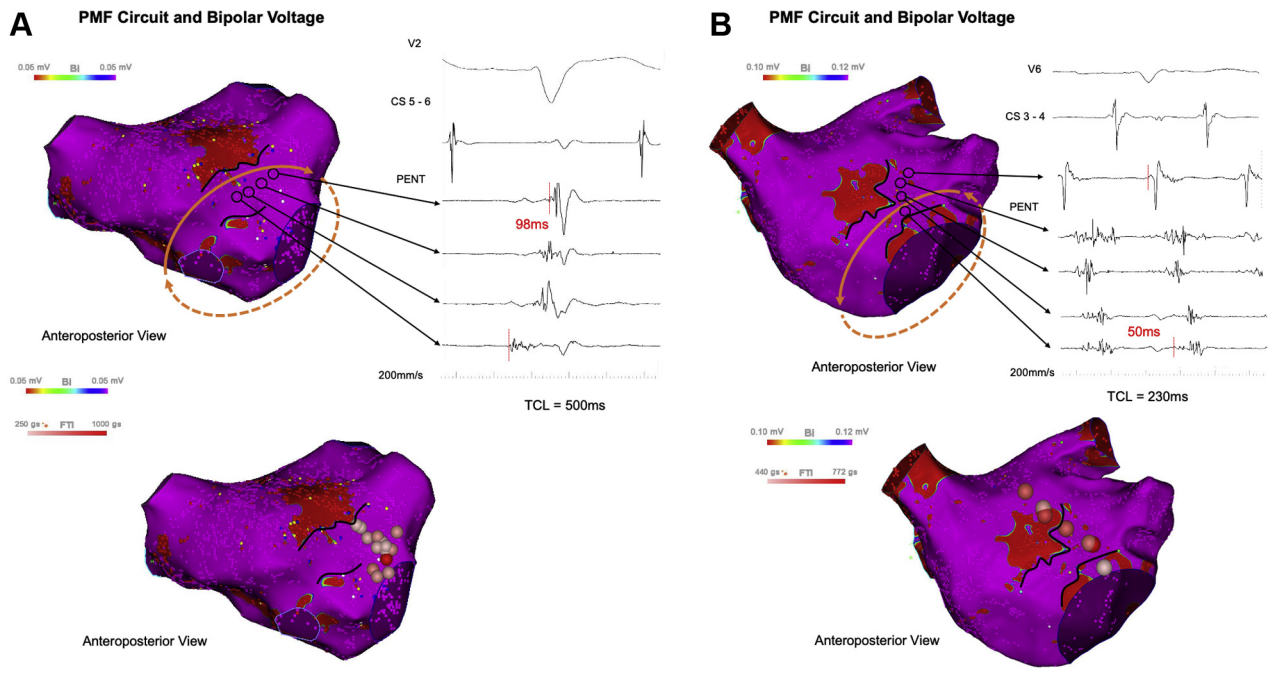

(A) The LA bipolar voltage map collected during PMF is shown in the **top panel**. The voltage limit is set at 0.05 mV after RM thresholding. **Black solid lines** indicate the nonconducting borders of the scar-related RM isthmus on the anterior LA wall. The **orange arrows** indicate direction of activation as seen on the RM (Video 4). The EGMs shown demonstrate the area within the isthmus that contains the most marked conduction delay (98 ms in this case). Ablation of the isthmus entrance led to PMF termination. **(B)** Following the same approach as in **A**, an anterior LA wall scar-related RM isthmus is demonstrated in a second patient without previous LA ablation. EGMs shown demonstrate the area within the isthmus that contains the most marked conduction delay (50 ms). This tachycardia was dual loop, with a second loop around the anterior wall scar. Tachycardia was terminated by ablation of the RM isthmus entrance. FTI = force time integral; LMIL = lateral mitral isthmus line; TCL = tachycardia cycle length; other abbreviations as in Figures 1 and 2.

The anatomic location of linear ablation performed (LMIL or SMIL) did not colocate with the retrospectively identified scar-related RM isthmus in 5 of 10 cases, where the LMIL or SMIL ablation did not transect the scar-related RM isthmus, supporting tachycardia. Figure 5 and Video 6 show an example of a case performed by using LAT mapping. The pattern of activation is diagnostic of PMF; however, because the bipolar voltage pattern cannot be appreciated, a constrained isthmus with defined boundaries related to LA scar is not apparent. Extensive LMIL ablation is pursued that does not terminate PMF. An SMIL line is additionally performed that terminates PMF. Analysis of the RM demonstrates an anterior wall scar-related isthmus that could have been initially targeted for ablation instead.

In 6 of 16 (36%) cases of linear ablation for PMF, a scar-related RM isthmus could not be identified. The mean ripple-defined bipolar voltage threshold for these 6 cases was not significantly different (0.17 ± 0.14 mV) from cases in which a critical isthmus was identified (0.13 ± 0.05 mV). Activation on the RM appeared rapid throughout the entire LA, without areas of critical slowing. A similar set of PMF where a slow conducting isthmus cannot be identified has been recently reported by other groups (18). In our group, 5 of these patients had previous PVI. One had previous LMIL ablation, with likely epicardial conduction over the ablated typical MI, and 1 had no previous LA ablation.

The anatomic locations of all 22 RM constrained isthmus sites supporting PMF are displayed on a schema of the LA in Figure 6. Table 3 summarizes the electrophysiological properties of all RM constrained isthmus sites.

FOLLOW-UP. A total of 26 patients completed follow-up for 15.5 ± 6.0 months; 2 were lost to follow-up (both had linear ablation). Electrocardiographic assessment had been performed in 20, with 6 assessed for symptoms of AT recurrence. There were 2 documented recurrences of AT >30 s in the 12

FIGURE 4 Anatomically Guided Linear Ablation

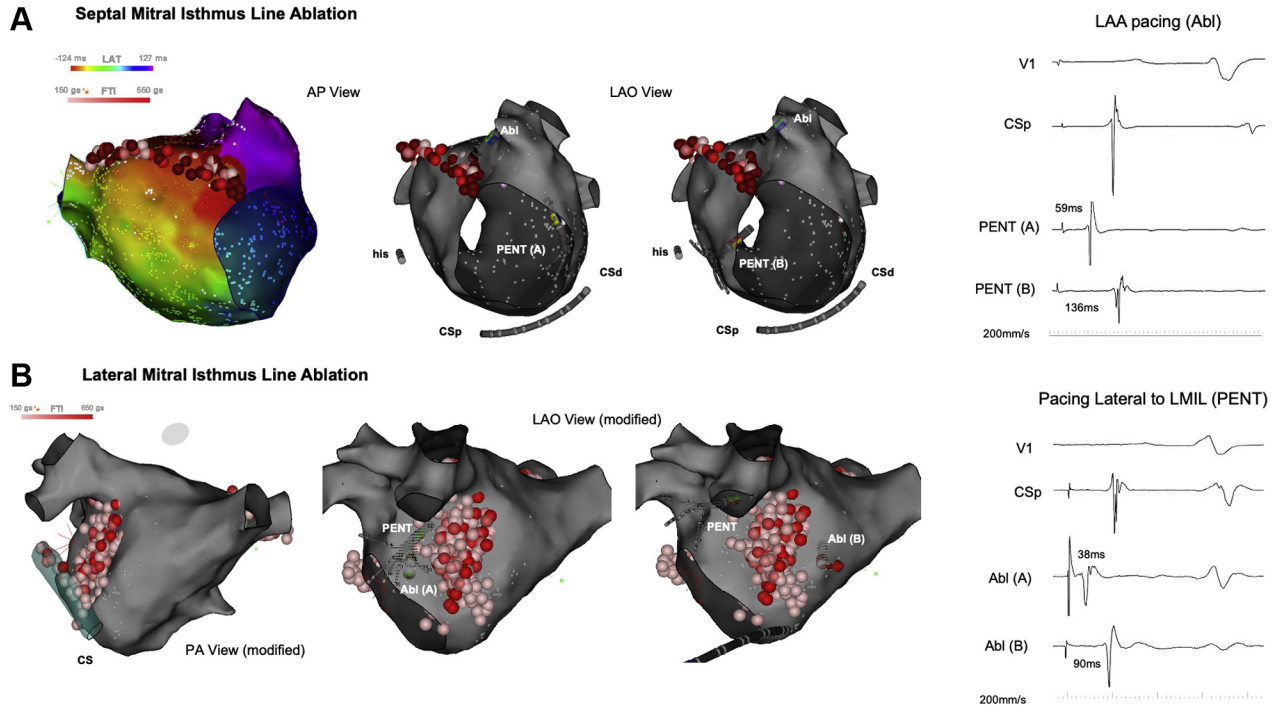

(A) The LAT map demonstrates PMF, rotating in a counterclockwise direction. An isthmus is not apparent because the early-meets-late site involves the entire anterior LA wall. An SMIL ablation is performed that terminated PMF. Conduction block is confirmed by pacing the LAA (ablation catheter) and demonstrating increasing activation time to the mapping catheter, which is initially positioned at the lateral LA wall (PENT A) and then the septal LA wall (PENT B). **(B)** An LMIL line is performed for PMF. Despite extensive ablation, including within and along the CS as shown, activation still travels from septal to lateral across the line. Pacing from the PentaRay catheter (Biosense Webster Inc., Irvine, California) lateral to the LMIL as shown results in increasing activation time to the mapping catheter as it is moved from septal (map A) to lateral (map B). LAT = local activation time; SMIL = septal mitral isthmus line; other abbreviations as in Figures 1 to 3.

patients who underwent RM scar-related isthmus ablation (17%). Both patients had previous LMIL ablation and a gap identified as the isthmus by using RM. This compared to 4 (3 documented, 1 symptomatic) recurrences of atrial arrhythmia in patients who underwent linear ablation at the lateral MI using LAT (29%)—all had previous circumferential pulmonary vein isolation, and 2 patients had previous LMIL ablation. The difference between recurrence rates was not statistically significant ($p = 0.65$).

DISCUSSION

In this study, we demonstrate that ablation of a scar-related isthmus identified by using RM can form the successful ablation target for PMF. In the group where ablation targeted a scar-related isthmus, tachycardia was terminated in all. In the group where linear ablation of an anatomic MI was performed, termination was achieved in only 63%. Retrospective review in these patients using RM was able to identify the electroanatomic characteristics of a scar-related isthmus in the majority of patients.

ELECTROANATOMIC CHARACTERISTICS OF THE PMF SCAR-RELATED ISTHMUS. In our study, the bipolar voltage values that defined LA scar and normal LA tissue were derived functionally on a circuit-by-circuit basis. By interpretation of the RM and bipolar voltage maps simultaneously, it was possible to accurately distinguish the spatial limits of nonconducting LA scar from critical areas of low voltage and slow conduction that formed the critical isthmus for PMF. We have previously described the superiority of RM over LAT mapping in a randomized trial, and the current study demonstrates that this is not simply due to diagnostic superiority but also being able to locate the critical isthmus as a better ablation target (17).

Overall, 22 scar-related isthmus sites were identified from 28 mapped PMF circuits. The scar-related

TABLE 2 Acute Procedural Outcomes

Ablation Outcome	Isthmus	Linear	p Value
RF termination	12/12 (100)	10/16 (63)*	0.027
Conduction block	11/12 (92)	11/16 (69)†	
RF applications	11.2 ± 6.0	30.8 ± 19.0	0.006
RF time, min	11.4 ± 5.3	26.2 ± 17.1	0.0004

Values are n/N (%) or mean ± SD. *With the first linear lesion set deployed for PMF. †LMIL, 71% (4 of 14) and SMIL, 83% (5 of 6).
PMF = perimitral flutter; RF = radiofrequency; other abbreviations as in Table 1.

isthmus was narrow (9.0 ± 6.2 mm), and its borders were defined by very-low-voltage tissue (0.12 ± 0.06 mV) that formed the nonconducting obstacles to activation that are required for re-entry. Activation through the isthmus proceeded slowly (~30 cm/s) compared to the normal LA (~70 cm/s). EGMs from within the isthmus were abnormal, of long duration, fractionated, and often spanned a significant portion of the mapped cycle length.

Distinction of the nonconducting tissue (scar) from very-low-voltage abnormal tissue (isthmus) based on activation mapping alone may be challenging because of annotation, interpolation, and window-of-interest limitations (19,20). In this study, we used RM to overcome these limitations and define areas of critical isthmus based on assessment of bipolar voltage and activation simultaneously. This process allowed reproducible identification of isthmus sites that could be targeted for ablation. **Figures 1 and 5** (Videos 1 and 6) illustrate this concept by demonstrating how LAT mapping may not always reveal the spatial limits of an isthmus to make targeted ablation easily feasible. To this end, CARTO3 has recently introduced an algorithm (extended early meets late) designed to improve distinction between areas of slow conduction that could suggest a scar-related isthmus and

FIGURE 5 Limitations of Local Activation Time Mapping

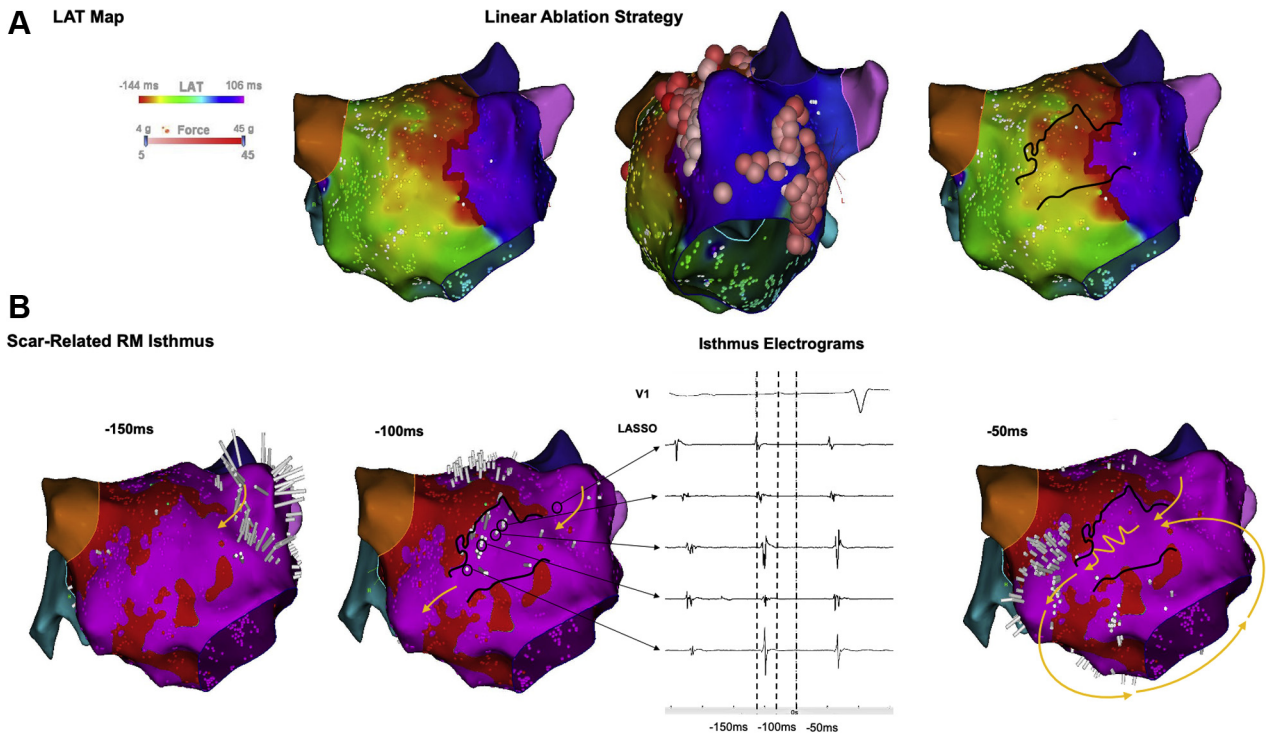

(A) LAT map of a counterclockwise PMF circuit. The early-meets-late site extends across the entire anterior LA wall. A linear lesion (LMIL) of the typical MI is initially performed that does not terminate PMF. A linear lesion (SMIL) of the anterior LA wall is performed that is successful. The scar-related RM isthmus is overlaid on the LAT map. The SMIL colocates with the isthmus; however, ablation is extensive and required 2 lesions sets to terminate tachycardia. **(B)** The RM and LA bipolar voltage maps of the same PMF are shown. After RM thresholding, the bipolar voltage limit is set at 0.20 mV. **Black solid lines** define the nonconducting borders of the RM isthmus. **Yellow arrows** demonstrate the direction of LA activation, as seen on the RM, during PMF. RM frames correspond to -150 ms, -100 ms, and -50 ms from the isthmus exit, as shown in the panel of EGMs. The RM isthmus contains 150 ms of the tachycardia, the cycle length of which is 400 ms. The RM isthmus provides a successful ablation target instead of pursuing linear ablation. Abbreviations as in Figures 1 to 4.

FIGURE 6 Schematic of Scar-Related Isthmus Sites

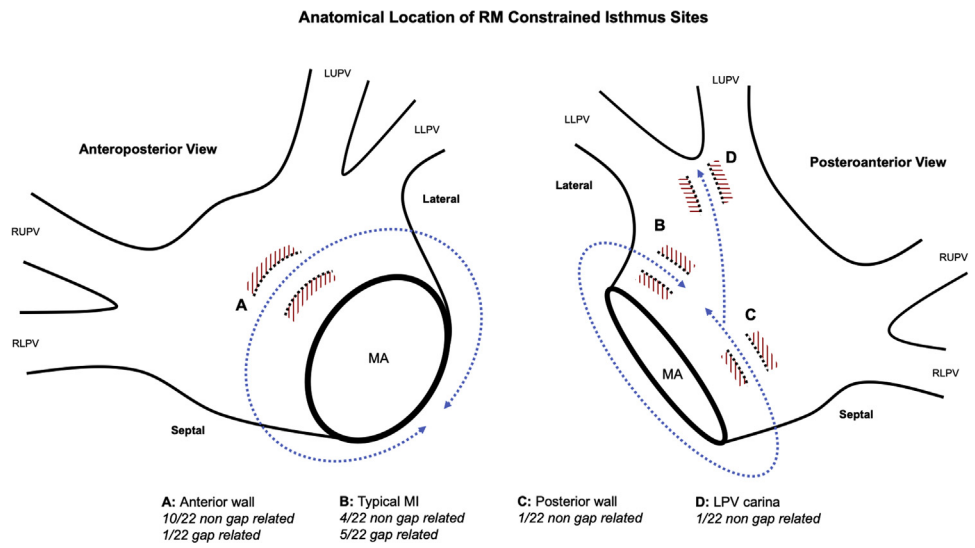

Anatomic locations of all 22 scar-related RM isthmus sites identified in this series. LLPV = left lower pulmonary vein; LPV = left pulmonary vein; LUPV = left upper pulmonary vein; MA = mitral annulus; RLPV = right lower pulmonary vein; RM = ripple mapping; RUPV = right upper pulmonary vein.

areas of block (projected as white lines) with LAT mapping. This system performed well in a recent validation study; however, the gold standard to which conduction block or delay was assessed was the ripple map (21). Our study supports this finding that RM appears to be the most effective method to locate the critical isthmus supporting AT.

The anterior wall of the LA was a common site for scar-related isthmus sites (10 of 22). Interestingly, 2 of these anterior wall isthmuses were mapped in patients who had no history of previous LA ablation. The exact reason for conduction slowing to permit macro-re-entry occurring more frequently on the anterior LA wall is, therefore, not clear and is not necessarily related to the presence of previous ablation lesions. The typical lateral MI segment, most commonly pursued for linear PMF ablation accounted for a minority (4 of 22) of scar-related RM isthmus sites. Whether LA scar, as determined using this approach, represents true scar from remodeling and fibrosis or areas of functional block cannot be determined by mapping 1 rhythm only, as we have previously described (21).

SCAR-RELATED ISTHMUS AS THE PMF ABLATION STRATEGY. Ablation of a scar-related isthmus was significantly more successful at terminating PMF than linear lesions (100% vs. 63%; p = 0.027). Furthermore, 25% of patients who underwent anatomic ablation for PMF required more than 1 linear lesion set. The extent and duration of ablation with linear lesions was almost 3 times greater than scar-related isthmuses, a statistically significant difference, given their larger length. This is important because extensive LA ablation is well known to be associated with pro-arrhythmia and recurrence (2,9). Even with extensive ablation, the rate of conduction block of any linear lesion in our study was 69%. This is similar to rates published in recent reports and is likely due to well-known anatomic challenges such as thick or long segments of myocardium needing ablation, cooling by nearby vascular structures, and LA

TABLE 3 Isthmus Site Characteristics (N = 22)

Mean bipolar voltage amplitude in nonfunctional tissue, mV	0.12 ± 0.06
Mean bipolar voltage amplitude in critical isthmus, mV	0.30 ± 0.09
Mean critical isthmus width, mm	9.0 ± 6.2
Mean critical isthmus conduction speed, cm/s	33.7 ± 15.0*
Normal LA mean conduction speed, cm/s	71.2 ± 21.5*
Anatomic location	
Gap in previous MI line	6/22 (27)
Anterior wall segment	10/22 (45)
Typical anatomic MI segment	4/22 (18)
Other	2/22 (10)

Values are mean ± SD or n/N (%). *p < 0.0001.
LA = left atrium; MI = mitral isthmus.

CENTRAL ILLUSTRATION **Two 3-Dimensional Electroanatomic Maps Displaying the 2 Different Ablation Strategies**

28 Patients Undergoing Catheter Ablation for Perimitral Flutter

12 Ripple Guided Scar-Related Isthmus Ablations

16 Anatomically Guided Linear Ablations

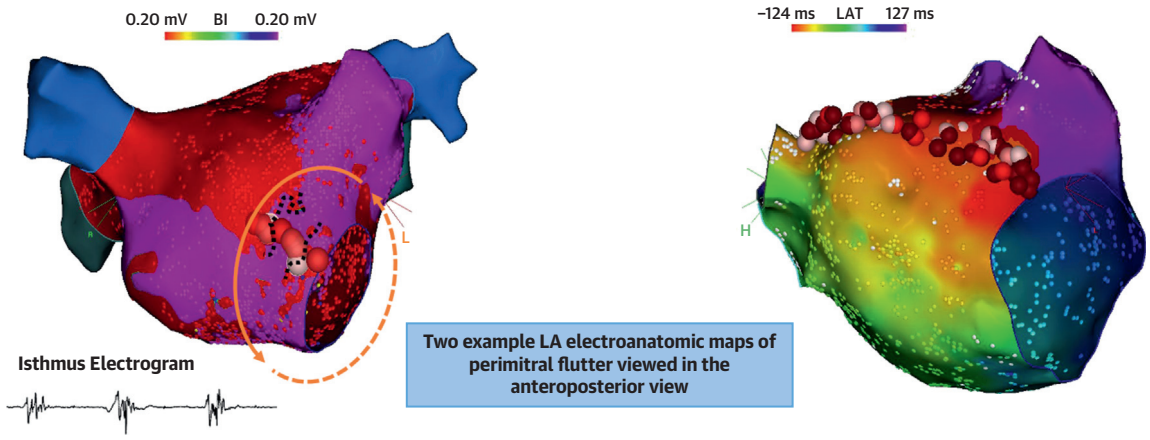

Two example LA electroanatomic maps of perimitral flutter viewed in the anteroposterior view

	Scar-Related Isthmus Ablation	Anatomically Guided Linear Ablation
Perimitral flutter termination	100%	63% (p = 0.027)
Ablation lesion block	92%	69%
Mean RF applications	11	31 (p = 0.006)

Katritsis, G. et al. J Am Coll Cardiol EP. 2021;7(5):578-90.

On the **left** is a bipolar voltage map of the left atrium, collected during perimitral flutter. On the **right** is a local activation time map from a different case. The bipolar voltage map limits have been determined using ripple mapping, and the **orange arrow** demonstrates the direction of ripple activation BI = bipolar voltage; LAT = local activation time.

epicardial conduction (9,22). However, the anatomic location of the linear ablation that was performed did not address the scar-related isthmus location 50% of the time. Two recent studies corroborate these findings; unlike our study, however, the definition of an isthmus is in 1 of these studies based on the voltage map alone and in the other is dependent on multiple operator-controlled factors (11,18). With RM, it is possible to identify specific isthmus sites within scar, defined per tachycardia, that are amenable to ablation by transection between the scar borders.

Given these limitations of anatomically guided linear ablation, RM PMF to identify scar-related isthmus sites to target appears to be a preferable strategy. A further conceptual reason to move away from anatomically guided linear ablation is the proarrhythmic effect of ablation scar, especially with linear lesions. In this study, we demonstrate that the critical isthmus location is variable. The anatomic location of the isthmus is largely dependent on the distribution of LA scar and low voltage that form the conduction obstacles and areas of conduction slowing that are required for macro-re-entry (23). Therefore, a pre-determined anatomic ablation line not only fails to address the critical isthmus but also generates a new arrhythmic substrate. This is not like typical cavotricuspid isthmus-dependent flutter, where blocking the anatomic isthmus is highly effective both acutely and in the long term.

STUDY LIMITATIONS. This study was retrospective with a small sample size and, therefore, susceptible to selection bias. It does, however, provide the justification for a prospective study of RM constrained isthmus ablation only. Determination of the RM bipolar voltage threshold for the LA during PMF is

dependent on the recording catheter and noise threshold of the entire recording system. Areas of poor EGM resolution may lead to false positive designation of conducting LA sites as scar. To attenuate this, cases had to be performed with the ConfiDense module on CARTO3.

CONCLUSIONS

PMF is easy to diagnose but difficult to ablate. RM is able to locate the critical isthmus and simplify the ablation process by avoiding empirical, anatomic linear lesions.

ACKNOWLEDGMENTS The authors acknowledge the help of Biosense Webster clinical support specialists Anushanth Balasundram, BSc, and Andrew Arnott, BSc, whose input was crucial for the completion of the electroanatomic map analysis. The group is part of the British Heart Rhythm Society Multi-Centre Trials Group. The Imperial College group is supported by British Heart Foundation Centre of Research Excellence and Grants and the National Institutes of Health (UK) Biomedical Research Centre.

FUNDING SUPPORT AND AUTHOR DISCLOSURES

This study was supported by a project grant from St. Mary's Coronary Flow Trust and a research grant from Biosense-Webster Inc. Imperial Innovations holds intellectual property relating to ripple mapping on behalf of Drs. Linton and Kanagaratnam, who have also received royalties from Biosense Webster. Drs. Luther, Jamil-Copley, Linton, and Kanagaratnam have received consulting fees with respect to ripple mapping from Biosense Webster. All other authors have reported that they have no relationships relevant to the contents of this paper to disclose.

ADDRESS FOR CORRESPONDENCE: Dr. Prapa Kanagaratnam, Department of Cardiology, Mary Stanford Wing, St. Mary's Hospital, Imperial College Healthcare NHS Trust, Praed Street, London W2 1NY, United Kingdom. E-mail: p.kanagaratnam@imperial.ac.uk.

PERSPECTIVES

COMPETENCY IN MEDICAL KNOWLEDGE: Perimitral flutter is a left atrial tachycardia that is commonly encountered in patients with previous ablation or left atrial scar tissue. Ablation is the most effective therapy and is usually performed by anatomically guided linear RF in the left atrium. We found that ablation directed to the specific scar-related isthmus critical for re-entry was more effective and that the specific electroanatomic mapping tool RM made identification of the scar-related isthmus more reliable.

TRANSLATIONAL OUTLOOK: Further studies are needed to assess whether a similar ripple-guided, scar-related isthmus can replace linear ablation lesions for all complex left atrial tachycardias.

REFERENCES

1. Ouyang F, Ernst S, Vogtmann T, et al. Characterization of reentrant circuits in left atrial macroreentrant tachycardia: critical isthmus block can prevent atrial tachycardia recurrence. Circulation 2002;105:1934–42.

2. Chae S, Oral H, Good E, et al. Atrial tachycardia after circumferential pulmonary vein ablation of atrial fibrillation: mechanistic insights, results of catheter ablation, and risk factors for recurrence. J Am Coll Cardiol 2007;50:1781–7.

3. Jais P, Shah DC, Haissaguerre M, et al. Mapping and ablation of left atrial flutters. Circulation 2000;101:2928–34.

4. Jais P, Hocini M, Hsu LF, et al. Technique and results of linear ablation at the mitral isthmus. Circulation 2004;110:2996–3002.

5. Hocini M, Shah AJ, Nault I, et al. Mitral isthmus ablation with and without temporary spot occlusion of the coronary sinus: a randomized clinical comparison of acute outcomes. J Cardiovasc Electrophysiol 2012;23:489–96.

6. Tzeis S, Luik A, Jilek C, et al. The modified anterior line: an alternative linear lesion in perimitral flutter. J Cardiovasc Electrophysiol 2010;21:665–70.

7. Ammar S, Luik A, Hessling G, et al. Ablation of perimitral flutter: acute and long-term success of the modified anterior line. Europace 2015;17:447–52.

8. Maurer T, Metzner A, Ho SY, et al. Catheter ablation of the superolateral mitral isthmus line: a novel approach to reduce the need for epicardial ablation. Circ Arrhythm Electrophysiol 2017;10:e005191.

9. Maheshwari A, Shirai Y, Hyman MC, et al. Septal versus lateral mitral isthmus ablation for treatment of mitral annular flutter. J Am Coll Cardiol EP 2019;5:1292–9.

10. Pathik B, Choudry S, Whang W, et al. Mitral isthmus ablation: a hierarchical approach guided by electroanatomic correlation. Heart Rhythm 2019;16:632–7.

11. Takigawa M, Derval N, Frontera A, et al. Revisiting anatomic macroreentrant tachycardia after atrial fibrillation ablation using ultrahigh-resolution mapping: implications for ablation. Heart Rhythm 2018;15:326–33.

12. Linton NW, Koa-Wing M, Francis DP, et al. Cardiac ripple mapping: a novel three-dimensional visualization method for use with electroanatomic mapping of cardiac arrhythmias. Heart Rhythm 2009;6:1754–62.

13. Jamil-Copley S, Linton N, Koa-Wing M, et al. Application of ripple mapping with an electroanatomic mapping system for diagnosis of atrial tachycardias. J Cardiovasc Electrophysiol 2013;24:1361–9.

14. Koa-Wing M, Nakagawa H, Luther V, et al. A diagnostic algorithm to optimize data collection and interpretation of ripple maps in atrial tachycardias. Int J Cardiol 2015;199:391–400.

15. Luther V, Linton NW, Koa-Wing M, et al. A prospective study of ripple mapping in atrial tachycardias: a novel approach to interpreting activation in low-voltage areas. Circ Arrhythm Electrophysiol 2016;9:e003582.

JACC: CLINICAL ELECTROPHYSIOLOGY VOL. 7, NO. 5, 2021
MAY 2021:578–90

16. Luther V, Cortez-Dias N, Carpinteiro L, et al. Ripple mapping: initial multicenter experience of an intuitive approach to overcoming the limitations of 3D activation mapping. J Cardiovasc Electrophysiol 2017;28:1285–94.

17. Luther V, Agarwal S, Chow A, et al. Ripple-AT study. Circ Arrhythm Electrophysiol 2019;12:e007394.

18. Yu J, Chen K, Yang B, et al. Peri-mitral atrial flutter: personalized ablation strategy based on arrhythmogenic substrate. Europace 2018;20:835–42.

19. De Ponti R, Verlato R, Bertaglia E, et al. Treatment of macro-re-entrant atrial tachycardia based on electroanatomic mapping: identification and ablation of the mid-diastolic isthmus. Europace 2007;9:449–57.

20. Del Carpio Munoz F, Buescher TL, Asirvatham SJ. Three-dimensional mapping of cardiac arrhythmias: what do the colors really mean? Circ Arrhythm Electrophysiol 2010;3:e6–11.

21. Iden L, Weinert R, Groschke S, Kuhnhardt K, Richardt G, Borlich M. First experience and validation of the extended early meets late (EEML) tool as part of the novel CARTO software HD COLORING. J Interv Card Electrophysiol 2021;60:279–85.

22. Luther V, Qureshi N, Lim PB, et al. Isthmus sites identified by Ripple Mapping are usually anatomically stable: A novel method to guide atrial substrate ablation? J Cardiovasc Electrophysiol 2018;29:404–11.

KEY WORDS atrial tachycardia, catheter ablation, electroanatomic mapping, isthmus, outcomes, perimitral flutter

APPENDIX For supplemental figures and videos, please see the online version of this paper.

Go to http://www.acc.org/jacc-journals-cme to take the CME/MOC/ECME quiz for this article.